Journal of Engineering Science and Technology
Vol. 13, No. 7 (2018) 2106 - 2124

DYNAMIC ANALYSIS OF TAPERED THIN-WALLED MASTS

KARIM S. NUMAYR[1], SULTAN T. MESMAR[1], MADHAR A. HADDAD[2,*]

[1]College of Engineering, American University of Madaba, P.O. Box 2882, Amman, Jordan
[2]Department of Architectural Engineering, United Arab Emirates University,
P.O. Box 15551, Al Ain, United Arab Emirates.
*Corresponding Author: madhar@uaeu.ac.ae

Abstract

Three methods are used to investigate the behaviour of cantilevered and linearly tapered thin-walled high masts under different kinds of dynamic loadings. First, the mast is represented as a single degree of freedom system with a prescribed shape function defining the mast deformation. Second, the finite element approach utilizing beam elements is used. Third, the governing partial differential equation of motion is solved using the finite difference approach. The effect of mesh density, load pattern, tapering ratio and height of masts on the behaviour of these masts is investigated. Results indicate that the finite difference method provides a better solution than the single degree of freedom and finite element methods. An increase in the taper ratio results in a decrease in the lateral displacements for both the concentrated and the distributed dynamic loadings. However, the increase in the taper ratio results in an increase in the lateral displacements during base motion. Masts with a high taper ratio experience lower natural frequencies than masts with a low taper ratio for the same material properties and height.

Keywords: Dynamic loads, Finite difference method, Finite element method, Tapered masts, Response.

1. Introduction

Knowledge of the behaviour of tapered, thin-walled, closed members subjected to lateral dynamic loads or base motion is important for the design of high masts, towers, and chimneys. As the height of these structures increases, their resistance against any type of loading becomes critical. Such structures may exhibit large deflections, especially if they are light and flexible. The large deflections may result in failure of the structure with possible consequential human and economic losses.

In general, any continuous structure has an infinite number of degrees of freedom and therefore an infinite number of natural frequencies and corresponding modal shapes. Resonance occurs when the structure is excited at a frequency that corresponds to its natural frequency. The response is a rapidly growing amplitude with time, requiring very little input energy, until either the structure fails by overstressing, or nonlinear effects limit the amplitude to a large value resulting in fatigue damage. Thus, analysis of the integrity of any structure should include determination of the natural frequencies and comparison of those frequencies with those from the time-dependent loading to which the structure will be subjected. Such analysis and comparison are essential to ensure that the frequencies imposed differ considerably from the natural frequencies in order to avoid resonance.

Krajcinovic [1] investigated cantilevered cylindrical shells subjected to wind loads. The adequacy of beam theory was questioned. A simple analysis was presented using semi-membrane theory, which was used to predict the axial membrane stress as a function of the shell geometry. However, Prabhu et al. [2] examined the adequacy of semi-membrane theory in a preliminary design and detected an error in Krajcinovic's analysis at the free end of the cylinder. Wang [3] studied a thin elastic rod held at one end in a strong crosswind, but ignored the effect of self-weight in the analysis.

Nakahira et al. [4] analysed the vibration of beams with varying cross-sections using the Stodola-Newmark method. The Stodola-Newmark is an alternative discrete approach to solve the governing ordinary differential equation directly. Nakahira et al. demonstrated the convergence and accuracy of the Stodola-Newmark method by solving several examples and comparing the results to those from analytical methods. Cleghorn and Tabarrok [5] and Rossi and Laura [6] compared the natural frequencies of vibration of linearly tapered beams with different combinations of edge supports. The natural frequencies are determined by the finite element algorithm using an element that accounts for the linear variation of the thickness, as opposed to having a uniform thickness. Rossi and Laura also studied the dynamic behaviour of linearly tapered beams.

Mulmule et al. [7] used a two-node beam element with two degrees of freedom per node to study the flexural vibration of rotating tapered Timoshenko beams. The effects of setting angle, hub radius, rotational speed and taper ratio on the flexural vibrations were studied. Cleghorn and Tabarrok [8] developed a tapered element model for the analysis of free vibration of linearly tapered Timoshenko beams. The shape functions are extracted from the homogeneous solution of the governing equation for the elastic deflections. Cleghorn and Tabarrok presented an example to demonstrate the performance of the tapered element. The results obtained using the proposed element were compared with results obtained from elements based on different finite element formulations. Nageswara and Venkateswara [9] studied the

applicability of static and dynamic criteria for the stability of a non-uniform cantilever column subjected to a tip concentrated sub tangential follower force.

Pirner and Fischer [10] studied the effect of wind-induced vibrations in TV towers with nonsymmetrical cross-sections. The height of the guyed TV masts and towers ranged between 15 m and 25 m. The interaction between bending and torsion was examined. The natural frequencies and the corresponding modal shapes were calculated based on finite element analysis. The experimental and theoretical natural frequencies were in good agreement. The axial displacement of the shaft was neglected in the analysis. Pirner and Fischer [11] assessed the service life of antennae towers and masts based on long-time monitoring data of wind and temperature. The rain-flow counting method and Miner's rule were used in the assessment. While temperature changes had a non-negligible effect on the service life of the GRP extensions, the effect of temperature on the service life was negligible compared to the wind effect.

Da Silva et al. [12] assessed structural models used in the analysis of transmission and telecommunication towers. Structural models commonly assume simple truss elements with hinged connections to model the towers. Two models were analysed. In the first model, the space beam and space truss elements were used to model the main structure and the bracing system, respectively. In the second model, space beam elements were used to model both the main structure and the bracing system. The heights of the towers analysed were 40 m and 75 m. Wind load and the self-weight of the components of the towers were considered in the analysis. The parametric study included the response, bending moments, stresses, natural frequencies and buckling loads of the towers. The results of the proposed models were in good agreement with, but less conservative than the simple truss analysis.

Yan-li et al. [13] used the discrete analysis method of random vibrations in analysing the wind-induced response of a guyed mast. The advantages of the frequency and time domain methods were combined. The vibration equation was discretized in the time domain. Mean square analysis was used to calculate the vibration response of the mast. As the higher order terms of displacements do not close but were considered in the analysis, Gaussian truncation was used to close the mean square equations. The response of a 150 m tall, guyed, ratio mast, determined with this discrete analysis method, was very close to the response obtained from the experimental results and the time domain method.

However, these papers say little about the behaviour of cantilevered and linearly tapered thin-walled closed members subjected to different types of dynamic loadings, such as the high masts being considered in this study. Hence, the analyses of the current problem will not only provide more data to the literature but will assist engineers as to a suitable method to use in the analysis, especially the finite difference analysis method.

The objective of the current study is to compare the behaviour of cantilevered and linearly tapered thin-walled high masts using the three analyses methods. Another objective is to show the behaviour of these masts under different types of lateral dynamic loadings, such as triangular distributed force, the concentrated force acting at the top of the mast, and a base motion. The triangular dynamic loading represents wind-induced forces. The concentrated load at the top of the mast represents cable-induced forces. The previous forces are separately applied during a limited duration of time. Damping is considered using an assumed

damping ratio. For several mast dimensions, computer programs are used to carry out all necessary calculations, such as the properties of the cross sections, numerical integrations, transverse deflections, fundamental natural frequencies, and the corresponding modal shapes. The models proved to be valid to give the results.

2. Problem Formulation and Methods of Solution

In order to have better insight into the response of high thin-walled masts, as shown in Fig. 1, subject to dynamic loading or base motion, three methods of analysis have been used. In the formulation process, the following basic assumptions were employed:

- The material is linearly elastic and the mast is homogeneous at any cross-section.
- The x - y plane is the principal plane of the mast. The x -axis, located along the mast neutral axis, undergoes no extension or contraction.
- Cross-sections perpendicular to the neutral axis, in the undeformed mast, remain plane and perpendicular to the deformed neutral axis (transverse shear deformation is neglected).
- σ_y and σ_z are negligible compared to the longitudinal stress of the mast, σ_x .
- Rotary inertia is neglected in the moment equation.

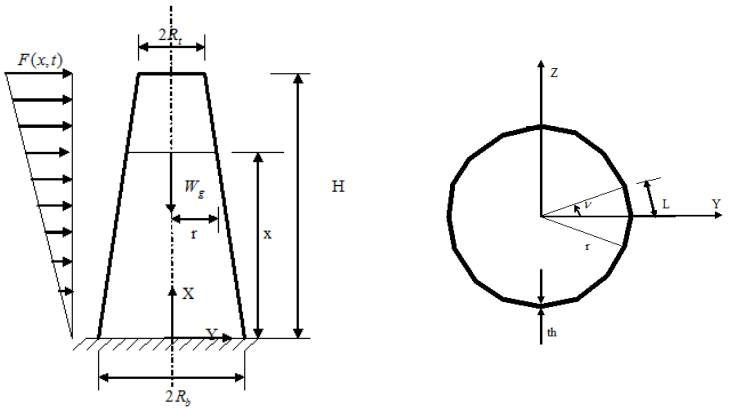

(a) Loading and geometry. **(b) Cross section (sixteen polygonal sides).**

Fig. 1. Schematic diagram of tapered thin-walled high mast.

2.1. Single degree of freedom system

The problem has an infinite number of degrees of freedom. However, a single degree of freedom analysis is possible provided that only a single deformed shape is developed during motion. Knowledge of the displacement of a single degree of freedom system determines the displacements of the entire system. Therefore, the displacement at any point, *x*, along the height of the mast is:

$$y(x,t) = \phi(x)Y(t) \tag{1}$$

where $\phi(x)$ is an assumed deformed shape of the cantilevered mast during the motion, given as:

$$\phi(x) = 1 - \cos(\pi x / 2H) \tag{2}$$

and $Y(t)$ is a function describing the displacement motion of the free end of the cantilevered beam (mast). $Y(t)$ is obtained by solving the differential equation of the equivalent system:

$$M\ddot{Y}(t) + C\dot{Y}(t) + K_C Y(t) = F(t) \tag{3}$$

where M and C are the generalized mass and damping coefficients. The generalized damping coefficient is taken as a ratio of the critical damping coefficient, which is equal to $2\sqrt{KM}$.

K_C is the combined generalized stiffness defined as the difference between the flexural stiffness, K, and the generalized geometric stiffness, K_G:

$$K_C = K - K_G \tag{4}$$

$$K = \int_0^H EI(x)(d^2y/dx^2)\,dx \tag{5}$$

$$K_G = \int_0^H N(x)(d\phi/dx)^2\,dx \tag{6}$$

where, $N(x)$ is the axial compressive force.

The generalized lateral force $F(t)$ is:

$$F(t) = \int_0^H P(x,t)\phi(x)\,dx \tag{7}$$

where, $P(x, t)$ is the lateral nodal force.

A Fortran 77 computer program was written to solve the single degree of freedom approach. The input variables are the bottom and top widths and thickness of the mast, the height of the mast, the number of polygonal sides, the damping ratio, the concentrated mass, the number of intervals within the integration limits, and the lateral dynamic loading function or base motion. The program consists of four main subroutines. First, subroutine MOMOINERT is used to calculate the moment of inertia and the cross-sectional area at any point along the height of the mast. Second, subroutine SIMPSN is used to calculate all necessary integrations needed for this method using the 1/3 Simpson rule. Third, subroutine FORCING is used to evaluate the forcing function at discrete data points in terms of length coordinates and time domain, to suit the next subroutine. Fourth, subroutine SOLVE is used to calculate the response of a simple damped oscillator excited by external force or by an acceleration acting at the support using Duhamel's integral principle. The response consists of the displacement, velocity, acceleration, and the support reaction.

2.2. Finite element method

The mast is divided into beam segments along the height. Equilibrium of forces at the nodes for each segment is:

$$[p_i] = [K_{ij}][\delta_i] \tag{8}$$

where $[p_i]$ and $[\delta_i]$ are the vectors of forces and displacements at node i, and $[K_{ij}]$ is the stiffness matrix of the beam element.

$$K_{ij} = \int_0^L EI\psi_i''(x)\psi_j''(x)\,dx \tag{9}$$

where $K_{ij} = K_{ii}$, according to Maxwell's reciprocal theorem, since the interchange of indices only requires the interchange of indices for $\psi_i(x)$ and $\psi_j(x)$.

L is the length of the beam segment and $\psi_i''(x)$ is the second derivative of the shape functions, corresponding to δ_i=1. The shape functions of the beam segment are:

$$\psi_1(x) = 1 - 3(x/L)^2 + 2(x/L)^3 \tag{10}$$

$$\psi_2(x) = x(1 - x/L)^2 \tag{11}$$

$$\psi_3(x) = 3(x/L)^2 - 2(x/L)^3 \tag{12}$$

$$\psi_4(x) = (x^2/L)((x/L) - 1) \tag{13}$$

The total deflection at coordinate x, due to arbitrary displacements at the nodal coordinates of the beam segment is given by superposition as:

$$y(x) = \sum_{i=1}^{4} \psi_i(x)\delta_i$$

The equivalent nodal forces of the element are:

$$P_i(x) = \int_0^L p(x,t)\psi_i(x)\,dx \tag{14}$$

The stiffness matrix of the element due to an axial force $N(x)$ is:

$$K_{Gij} = \int_0^L N(x)\psi_i'(x)\psi_j'(x)\,dx \tag{15}$$

The global stiffness matrix of the mast is obtained by assembling the element stiffness matrices of the mast for the flexural and axial cases. The combined stiffness matrix of the mast is:

$$[K_c] = [K] - [K_G] \tag{16}$$

The static lumped mass concept is used. The mass of each element is distributed to the nodes of the element. The inertial effect associated with the rotational degree of freedom is assumed to be zero.

A computer program was constructed utilizing Fortran 77 to serve the multi-degree of freedom system using the finite element approach. In addition to the input variables of the single degree of freedom system, the following input variables are

used: the number of elements, the number of degrees of freedom, the number of reduced coordinates, the initial time, the final time under consideration, the number of divisions in the time domain, the number of divisions along the mast, and the lateral dynamic loading function or base motion. The computer program consists of five main subroutines. The first and second subroutines are the Simpson and the MOMOINERT. The third subroutine, JACOBI, is an iterative numerical method, which is used to calculate the eigenvalues and the corresponding eigenvectors for the multi-degree of freedom system. The fourth subroutine, CONDE, is used to reduce the first P nodal coordinates by static condensation and to calculate the reduced stiffness, mass and transformation matrices. The fifth subroutine, MODAL, is designed to give the response of a multi-degree of freedom system using the modal superposition method. The last three subroutines are adopted from Paz [14].

2.3. Finite difference method

A non-uniform beam has both a mass per unit length, $m(x)$, and the moment of inertia, $I(x)$, depending on the length coordinate, x. Hence, the partial differential equation (P.D.E.) according to Bernoulli-Euler beam theory is:

$$(\frac{\partial^2}{\partial x^2})(EI(x)(\frac{\partial^2 u(x,t)}{\partial x^2})) + m(x)(\frac{\partial^2 u(x,t)}{\partial t^2}) = P(x,t) \tag{17}$$

Equation (17) is solved using the finite difference method by substituting the central difference derivatives of the displacements in the P.D.E. For example, at the point of intersection of the *ith* and *kth* divisions shown in Fig. 2, the solution is:

$$\begin{aligned} &E(\frac{1}{\Delta x^4})[(I_{i+1} - 2I_i + I_{i-1})(u_{i+1,k} - 2u_{i,k} + u_{i-1,k}) + 0.5(I_{i+1} - I_{i-1})(u_{i+2,k} \\ &- 2u_{i+1,k} + 2u_{i-1,k} - u_{i-2,k}) + I_i(u_{i+2,k} - 4u_{i+1,k} + 6u_{i,k} - 4u_{i-1,k} + u_{i-2,k})] + \\ &m_i(\frac{1}{\Delta t^2})[u_{i,k+1} - 2u_{i,k} + u_{i,k-1}] = P_{i,k} \end{aligned} \tag{18}$$

The boundary conditions are considered as functions of displacement, x, and time, t. For instance, in the x-direction, the boundary conditions in discrete form are: $u_{0,k} = 0$ (displacement = 0) and $u_{-1,k} = u_{1,k}$ (slope = 0), at the fixed end of the mast, $x = 0$. At the same time, for the x-direction the boundary conditions are: $u_{i+1,k} = 2u_{i,k} - u_{i-1,k}$ (moment = 0) and $u_{i+2,k} = 4u_{i-i,k} - 4u_{i-1,k} + u_{i-2,k}$ (shear = 0) at the free end of the mast, $x = L$.

In the t-direction, the boundary conditions are: $u_{i,0} = 0$ (displacement = 0) and $u_{i,1} = u_{i,-1}$ (velocity = 0) at the initial time, $t = 0$. There is no information beyond the end of the time of interest, $t = T$. Therefore, the backward finite difference is used in order to avoid dealing with fictitious points of no obvious relation. The finite difference formula with second-order error is:

$$\frac{\partial^2 u_{i,k}}{\partial t^2} = (\frac{1}{\Delta t^2})(2u_{i,k} - 5u_{i,k-1} + 4u_{i,k-2} - u_{i,k-3}) \tag{19}$$

The above boundary conditions are used to find the relations for all the fictitious points in line with the points inside the network. The resulting sets of algebraic equations are solved for the displacement at each node in the network at different time increments.

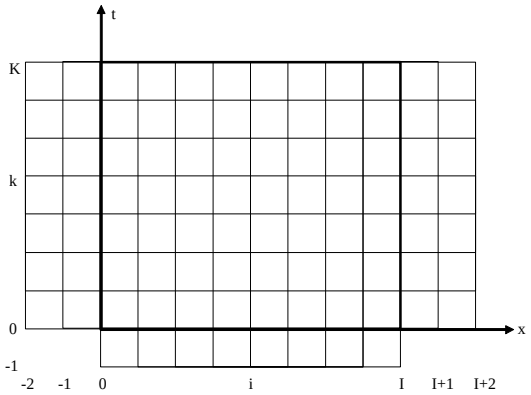

Fig. 2. Network of the length of the mast and time used in the finite difference method.

A Fortran 77 computer program was constructed for this purpose. Subroutine GAUSS is used to calculate all the necessary integrations. The input variables are half the top and half the bottom widths, the thickness of the thin-walled mast, the number of polygonal sides, the length of the mast, the number divisions along the height of the mast, the final time under consideration, the number of divisions in the time domain, and the type of forcing function.

3. Results and Discussion

A wide variety of linearly tapered cantilever thin-walled members have been analysed under different types of dynamic loadings in line with the different methods of analysis. The thin-walled members are made of steel and have polygonal cross-sections. The modulus of elasticity of steel used in the analyses is 200 GPa and the density of steel is 7850 kg/m^3. The height of the mast is 40 m and the wall thickness 0.006 m. The number of polygon sides is 16 as shown in Fig. 1(b). The width of the base of the mast is 1.5 m. The tapering ratio varies between 0 and 1.0. The tapering ratio of the mast is defined as the ratio of the top to bottom widths of the mast. A triangularly distributed load is applied along the height of the mast in the lateral direction as shown in Fig. 1(a).

$$F(x,t) = (\frac{1.5x}{H})\sin(4\pi t) \quad \text{kN/m} \tag{20}$$

where x and t are the distance from the base of the mast and the duration of the applied force, respectively. H is the height of the mast.

A concentrated load is applied at the free end of the mast in the lateral direction:

$$F(t) = 20\sin(4\pi t) \quad \text{kN} \tag{21}$$

The ground motion acceleration function is applied at the base of the mast in the lateral direction:

$$F(t) = 0.25g \sin(4\pi t) \quad \text{m/s}^2 \tag{22}$$

3.1. Effect of method of solution

The lateral deflections versus the height of the mast are shown in Figs. 3(a), (b) and (c). The tapering ratio of the mast is 0.4. The lateral deflections of the mast, shown in Fig. 3(a), are determined by representing the mast as a single degree of freedom system. The deflected shape represents the first modal shape.

The lateral deflections of the mast, shown in Fig. 3(b), are determined using the finite element method. Thirty-two finite elements are used along the height of the mast. The deflected shapes of the mast have several inflexions across the height during motion. The mast is represented as a multi-degree of freedom system. Therefore, the deflected shape is a combination of several modal shapes.

The lateral deflections of the mast, shown in Fig. 3(c) are determined using the finite difference method. Thirty-two divisions, along with the height of the mast and twenty divisions during the time duration, are used in the finite difference analysis. The deflected shapes of the mast are smooth and represent the behaviour of a continuous system.

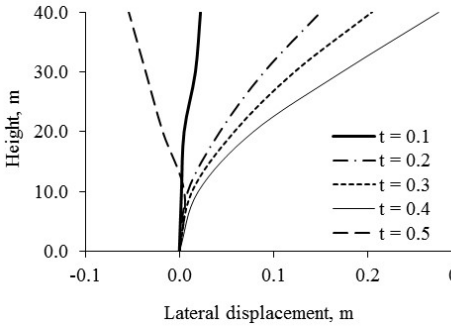

(a) Single degree of freedom method.

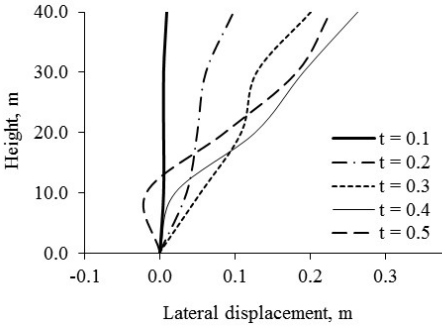

(b) Finite element method.

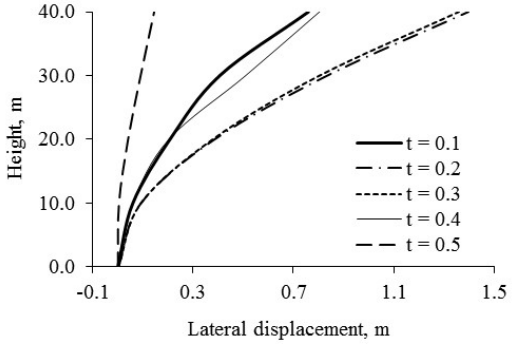

(c) Finite difference method.

Fig. 3. Lateral displacement along the height of the mast using three analysis methods.

3.2. Effects of mesh density

The effect of increasing the number of divisions in the time domain on the difference in the lateral deflections between the finite element method and finite difference method are shown in Figs. 4(a) through 4(d). Four, eight, sixteen and thirty-two elements are used along the height of the mast. The number of divisions, in the time domain is between 5 and 20. Different tapering ratios (0.2, 0.4, 0.6, and 0.8) are used. Increasing the number of elements along the height of the mast, and/or increasing the number of divisions in the time domain results in reducing the difference between the lateral deflections using the finite element and finite difference methods and improves the solution. The effect of increasing the number of elements along the height of the mast is more pronounced for tapering ratios below 0.6. The number of divisions in the time domain becomes more critical for tapering ratios above 0.6. The finite difference method is sensitive to the number of divisions in the time domain. As the tapering ratio increases, the difference between the lateral deflections using the finite element and finite difference methods decreases for a constant number of divisions along the height of the mast, and during the same time interval.

The effect of increasing the number of divisions in the time domain, on the difference of the lateral deflections between the finite element and finite difference methods, is shown in Fig. 5. The lateral deflections are compared at the top of the mast. Four elements are used along the height of the mast. The tapering ratio of the mast is 0.4. The results are captured at a time of 0.5 seconds for the distributed, concentrated dynamic loadings and base motion. Increasing the number of divisions in the time domain improves the solution, especially for the concentrated load case. The difference in the lateral deflections is higher for the concentrated load case than the difference for the other loading cases. The mesh density is not sufficient to translate the effect of the concentrated load through the nodal points. Therefore, a finer mesh is needed to improve the solution for the concentrated load case.

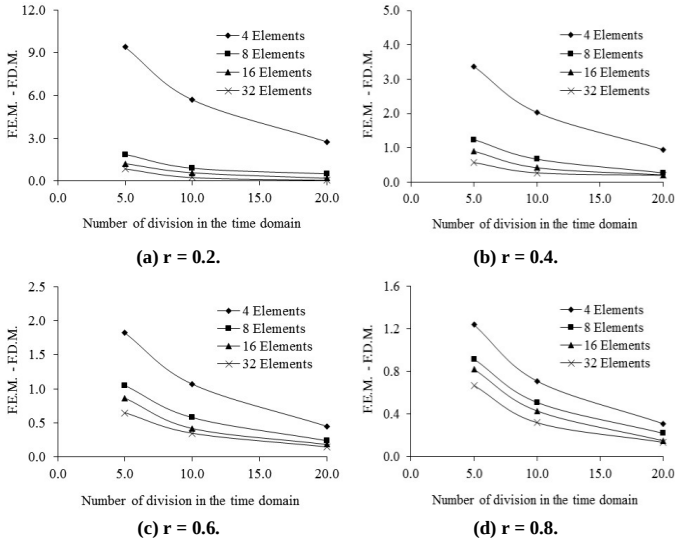

Fig. 4. Effect of increasing the number of divisions, in the time domain on the difference in the lateral displacements between the finite element method and the finite difference method.

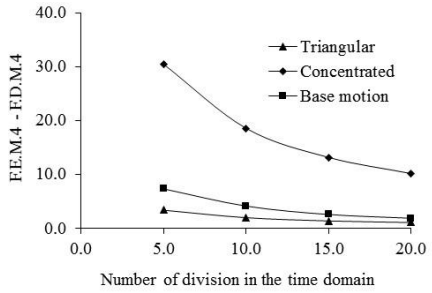

Fig. 5. Effect of increasing the number of divisions, in the time domain, on the difference in the lateral displacements between the finite element method and the finite difference, for different types of dynamic loadings.

The effect of increasing the number of elements along the height of the mast on the lateral displacement at the top of the mast is shown in Fig. 6. The lateral displacements are compared using the finite element and finite difference methods. This comparison is held for twenty divisions in the time domain at a time period of 0.5 seconds for the triangular loading case. The tapering ratio of the mast is 0.6. Increasing the number of elements above sixteen along the height of the mast improves the solution, according to the finite element method. Comparatively, increasing the number of divisions along the mast improves the solution according to the finite difference method, to a certain extent.

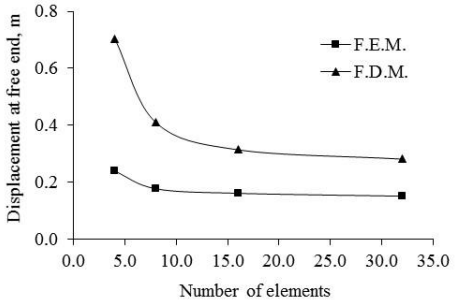

Fig. 6. Effect of increasing the number of elements, along the height of the mast, on the lateral displacement at the top end of the mast.

3.3. Effect of load pattern

The mast is separately subjected to three different types of dynamic loadings. The height of the mast is 40 m. The tapering ratio of the mast is equal to 1.0. The analysis is carried out at time level equal to 0.3 seconds.

3.3.1. Distributed dynamic triangular load applied along the height of the mast

The lateral displacements versus the height of the mast for the distributed dynamic load are shown in Fig. 7(a). The different methods of analysis are used to obtain the displacements, which are compared with the exact solution. The single degree of freedom approach underestimates the exact results. The best solution is achieved by using the finite difference method with a mesh density of 32 divisions along the height of the mast, and 20 divisions in the time domain. The finite element results are close to the exact solution for the lower part of the mast (height less than 10 m).

However, the finite element analysis overestimates the exact solution for the upper part of the mast. The number of elements, along the height of the mast in the finite element analysis, is 32. It is recommended to increase the number of divisions, in the time domain, above 20, to improve the finite difference solution.

3.3.2. Concentrated dynamic load applied at the top of the mast

The lateral displacements versus the height of the mast for the concentrated dynamic load are shown in Fig. 7(b), for the different methods of analysis. The lateral displacements are compared with the exact solution. The single degree of freedom approach underestimates the exact results again. As above, the best solution is achieved by using the finite difference method with a mesh density of 32 elements along the height of the mast, and 20 divisions in the time domain. The finite element analysis provides close results to the exact solution for the lower half of the mast (height below 20 m). The finite element analysis overestimates the exact results for the upper half of the mast. Thirty-two elements are used in the finite element analysis along the height of the mast. To improve the finite difference results, using 32 divisions along the height of the mast, it is recommended to increase the number of divisions in the time domain above 20.

3.3.3. Ground motion applied at the base of the mast

The lateral deflections versus the height of the mast for the applied ground motion are shown in Fig. 7(c), for the different methods of analysis. The lateral deflections are compared with the exact solution. The closest solution to the exact one is given by the single degree of freedom approach. The finite difference approach underestimates the deflections. The finite element approach using 32 elements provides results closer to the exact than the finite difference approach. The finite difference method using 32 divisions along the mast and 15 divisions in the time domain did not provide good results as in the previous cases. This is due to the low number of divisions in the time domain.

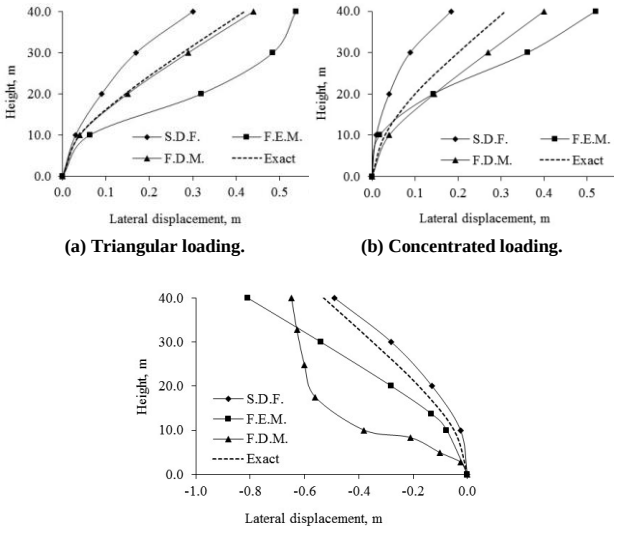

(a) Triangular loading. **(b) Concentrated loading.**

(c) Base motion.

Fig. 7. Lateral displacement along the height of the mast using different methods of analyses for $r = 1$.

3.4. Effect of the geometric parameters of the mast

The effect of increasing the tapering ratio on the lateral displacement of the masts using different methods of analyses under different types of dynamic loadings is investigated here. In addition, the effect of increasing the tapering ratio and height on the natural frequency of the masts is presented.

3.4.1. Tapering ratio of the mast

The lateral displacements using sixteen finite elements along the height of the mast are shown in Fig. 8(a). The tapering ratios of the mast are equal to 0.0, 0.2, 0.4, 0.6, 0.8, and 1.0. The mast is subjected to the triangular dynamic load along the height. The analysis is captured at a time of 0.3 seconds. Increasing the tapering ratio decreases the lateral deflections of the mast. The high load concentration at the top affects the lowest stiffened part of the cantilever.

The lateral displacements along the height of the mast are shown in Fig. 8(b) using the finite difference method. Eight divisions are used along the height of the mast, and 25 divisions in the time domain. The tapering ratios of the mast are 0.2, 0.4, 0.6, 0.8, and 1.0. The concentrated dynamic load is applied at the top of the mast. The dashed lines represent the proposed deflected shape, 1.0 - cos($\pi x/2H$), for the generalized coordinates as a single degree of freedom system. Increasing the tapering ratio decreases the lateral deflections of the mast. The difference in the lateral deflections for the concentrated dynamic load case is greater than that for triangular dynamic loading case for tapering ratio below 0.6.

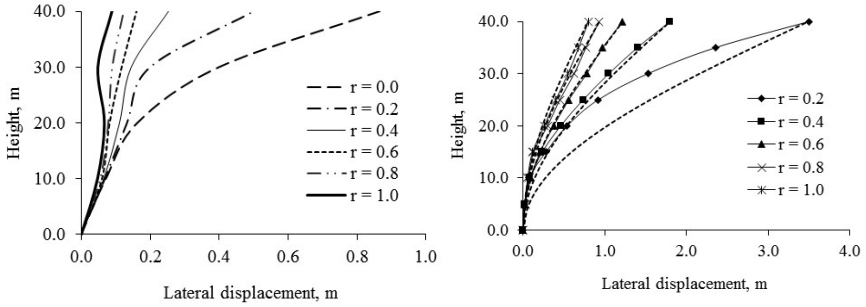

(a) Finite element method. **(b) Finite difference method.**

Fig. 8. Lateral displacement along the height of the mast for different tapering ratios.

The lateral displacements at the free end of the cantilever, during the time of loading, are shown in Fig. 9(a) through 9(e). The tapering ratios of the mast are 0.2, 0.4, 0.6, 0.8 and 1, respectively. Three different methods are used in the analyses. The finite element method is used with 32 elements along the height of the mast. The finite difference method is used with a mesh size of 32 divisions, along with the height of the mast, and 25 divisions in the time domain. The differences in the lateral displacements between the finite element and finite difference methods increase for low tapering ratios. It is necessary to

increase the number of divisions in the time domain in order to improve the solution of the finite difference to compensate for the large differences such as the case shown in Fig. 9(a) for a tapering ratio of 0.2. In general, the single degree of freedom analysis provides the lowest values of displacements. The finite element results are less than the single degree of freedom results, in some cases, for times of loading greater than 0.42 seconds.

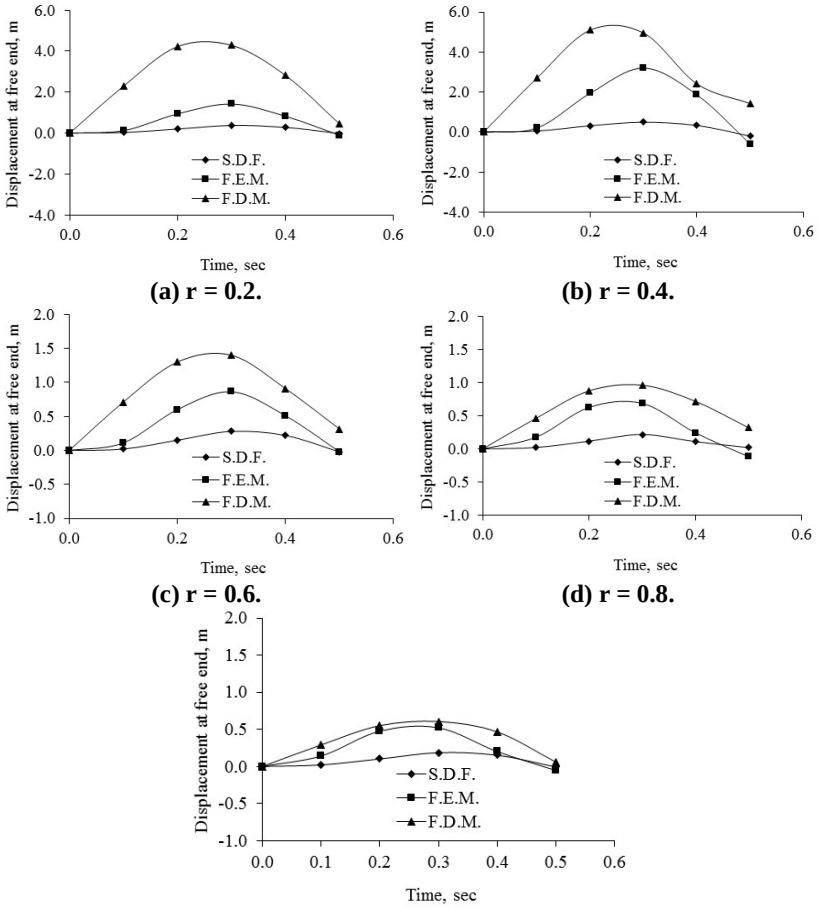

(a) r = 0.2. **(b) r = 0.4.**

(c) r = 0.6. **(d) r = 0.8.**

(e) r = 1.

Fig. 9. Lateral displacement versus time, at the free end of the mast, using different methods of analyses, for different tapering ratios.

The lateral displacements at the top of the mast are shown in Fig. 10 during the time of the ground motion. Thirty-two elements are used along the height of the mast. The tapering ratios of the mast are 0.2, 0.4, 0.6, 0.8, and 1.0. The tapering ratio has no noticeable influence on the lateral deflections up to approximately 0.3 seconds. Beyond this limit, a small effect appears and starts propagating. Increasing the tapering ratio increases the lateral deflection at time of 0.5 seconds. This occurs because the ground motion is acting directly at the base of the mast and the base is the stiffest part of the mast. The excitation translates weakly from the bottom to the

top of the mast. Therefore, the structure is more stable against the base motion as the tapering ratio decreases.

The effect of increasing the tapering ratio on the difference between the finite element and finite difference methods is shown in Fig. 11. Four elements are used along the height of the mast. Twenty divisions are used in the time domain for the finite difference analysis. Three types of different dynamic loadings are used. The best results are achieved for the triangular loading case. The type of loading has an influence on the convergence of the finite difference method. For example, the concentrated load needs a larger network than the base motion or the distributed load. Increasing the tapering ratio leads to faster convergence in the solution, for all loading cases.

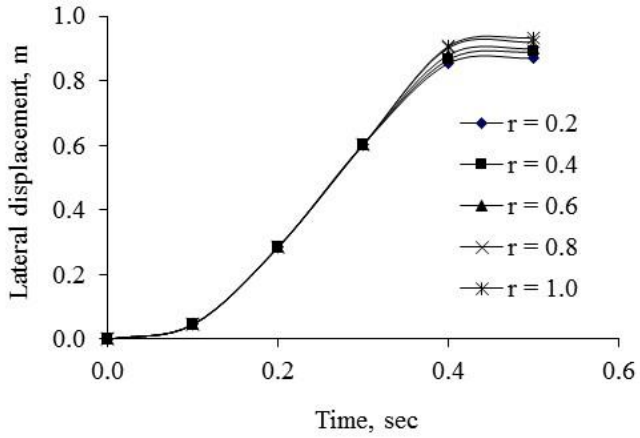

Fig. 10. Lateral displacement versus time, at the free end of the mast, for different tapering ratios.

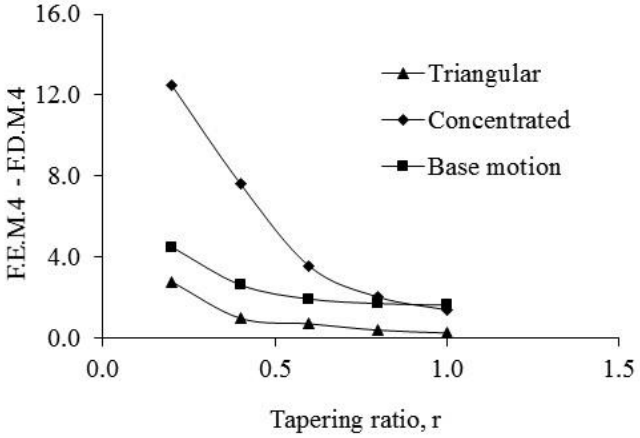

Fig. 11. Effect of increasing the tapering of the mast on the difference in the lateral displacement between the finite element method and the finite difference method.

The effect of increasing the tapering ratio on the natural frequency of the mast is shown in Fig. 12. The increase in the tapering ratio results in a decrease of angular natural frequency of the mast.

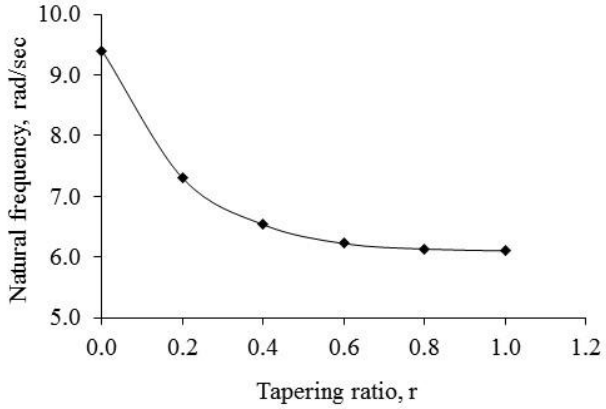

Fig. 12. Effect of increasing the tapering of the mast on its natural frequency.

3.4.2. The height of the mast

The effect of increasing the height on the natural frequency of the mast is shown in Fig. 13. The height of the mast result in a decrease in the natural frequency of the mast.

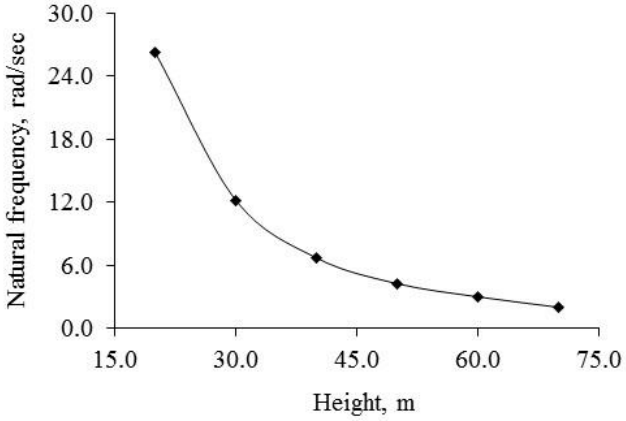

Fig. 13. Effect of increasing the height of the mast on its natural frequency.

4. Conclusions and Recommendations

Based on the results discussed above, the following conclusions are drawn:

- The best method for the analysis of tapered thin-walled masts is the finite difference method. However, a fine mesh both along the length of the mast and in the time domain is recommended.
- Increasing the tapering ratio results in a decrease in the lateral displacements for both the concentrated and the distributed dynamic loading. However, increasing the tapered ratio results in an increase in the lateral displacement during ground motions.
- Masts with a high taper ratio experienced lower natural frequencies than masts with a low taper ratio for the same material properties and height.
- Tall masts have a lower natural frequency than short masts of the same material and geometric properties.
- The effect of increasing the number of polygonal sides on the lateral deflection of high thin-walled masts, subjected to dynamic loads or ground motion, is negligible and cannot be seen from the results for this case of study.
- It is recommended to use other elements such as shell elements in the finite element solution.
- It is recommended to improve the finite difference solution by replacing the Gauss solver of the system of equations by another faster one such as the column solver.

Acknowledgement

The authors gratefully acknowledge the technical help of the staff at the computer centre at the Jordan University of Science and Technology.

Nomenclatures

C	Generalized damping coefficient
$F(t)$	Generalized lateral force
g	Gravitational acceleration
H	Height of the mast
$I(x)$	Moment of inertia
K	Flexural stiffness
K_C	Combined generalized stiffness
K_G	Generalized geometric stiffness
$[K_{ij}]$	Stiffness matrix of the beam element
L	Length of the beam segment
M	Generalized mass coefficient
$M(x)$	Mass per unit length
$N(x)$	Axial force
$P(x, t)$	Lateral nodal force
$[p_i]$	Vector of forces at node i
t	Time
u	Displacement
$Y(t)$	A function describing the displacement motion

Greek Symbols

$[\delta_i]$	Vector of displacements at node i
$\phi(x)$	Assumed deformed shape
$\psi_i(x)$	Shape function
$\psi_i^{"}(x)$	Second derivative of the shape function
σ	Stress

Abbreviations

PDE	Partial differential equation

References

1. Krajcinovic, D. (1970). Semimembrane analysis of cylindrical shells subjected to wind loading. *Journal of Applied Mechanics*, 37(4), 995-1001.
2. Prabhu, K.S.; Goplacharynlu, S.; and Johns, D.J. (1975). Cantilever cylindrical shells subjected to wind loading. *Journal of Applied Mechanics*, 42(1), 233-234.
3. Wang, C.Y. (1989). Cantilever rod in cross wind. *Journal of Applied Mechanics*, 56(3), 369-643.
4. Nakahira, N.; Ozawa, K.; and Mizusawa, T. (1992). Vibration of beams with variable cross-sections by the Stodola-Newmark method. *Computers and Structures*, 43(5), 999-1004.
5. Cleghorn, W.L.; and Tabarrok, B. (1992). Finite element formulation of a tapered Timoshenko beam for free lateral vibration analysis. *Journal of Sound and Vibration*, 152(3), 461-470.
6. Rossi, R.E.; and Laura, P.A.A. (1993). Numerical experiments on vibrating, linearly tapered Timoshenko beams. *Journal of Sound and Vibration*, 168(1), 179-183.
7. Mulmule, S.; Singh, G.; and Venkateswara Rao, G. (1993). Flexural vibration of rotating tapered Timoshenko beams. *Journal of Sound and Vibration*, 160(2), 372-377.
8. Cleghorn, W.L.; and Tabarrok, B. (1992). Finite element formulation of tapered Timoshenko beam for free lateral vibration analysis. *Journal of Sound and Vibration*, 152(3), 461-470.
9. Nageswara Rao, B.; and Venkateswara Rao, G. (1990). Stability of tapered cantilever columns subjected to a tip-concentrated follower force with or without damping. *Computers and Structures*, 37(3), 333-342.
10. Pirner, M.; and Fischer, O. (1996). Wind-induced vibrations of nonsymmetrical structures. *Journal of Wind Engineering and Industrial Aerodynamics*, 65(1-3), 63-75.

11. Pirner, M.; and Fischer, O. (1999). Long-time observation of wind and temperature effects on TV towers. *Journal of Wind Engineering and Industrial Aerodynamics*, 79(1), 1-9.
12. da Silva, J.G.S.; Vellasco, P.C.G.; de Andrade, S.A.L.; and de Oliveira, M.I.R. (2005). Structural assessment of current steel design models for transmission and telecommunication towers. *Journal of Constructional Steel Research*, 61(8), 1108-1134.
13. Yan-li, H.; Xing, M.; and Zhao-min, W. (2003). Nonlinear discrete analysis method for random vibration of guyed masts under wind load. *Journal of Wind Engineering and Industrial Aerodynamics*, 91(4), 513-525.
14. Paz, M. (1991). *Structural dynamics theory and computations.* Dallas: Chapman and Hall.